Photosynth Res
DOI 10.1007/s11120-017-0444-1

ORIGINAL ARTICLE

Loss of LHCI system affects LHCII re-distribution between thylakoid domains upon state transitions

Mauro Bressan[1] · **Roberto Bassi**[1] · **Luca Dall'Osto**[1]

Received: 12 April 2017 / Accepted: 12 September 2017

Abstract LHCI, the peripheral antenna system of Photosystem I, includes four light-harvesting proteins (Lhca1-Lhca4) in higher plants, all of which are devoid in the *Arabidopsis thaliana* knock-out mutant *ΔLhca*. PSI absorption cross-section was reduced in the mutant, thus affecting the redox balance of the photosynthetic electron chain and resulting in a more reduced PQ with respect to the wild type. *ΔLhca* plants developed compensatory response by enhancing LHCII binding to PSI. However, the amplitude of state transitions, as measured from changes of chlorophyll fluorescence in vivo, was unexpectedly low than the high level of PSI–LHCII supercomplex established. In order to elucidate the reasons for discrepancy, we further analyzed state transition in *ΔLhca* plants. The STN7 kinase was fully active in the mutant as judged from up-regulation of LHCII phosphorylation in state II. Instead, the lateral heterogeneity of thylakoids was affected by lack of LHCI, with LHCII being enriched in stroma membranes with respect to the wild type. Re-distribution of this complex affected the overall fluorescence yield of thylakoids already in state I and minimized changes in RT fluorescence yield when LHCII did connect to PSI reaction center. We conclude that interpretation of chlorophyll fluorescence analysis of state transitions becomes problematic when applied to mutants whose thylakoid architecture is significantly modified with respect to the wild type.

Keywords Chloroplast · Photosystem I · LHCI · LHCII · State transitions · Grana · Stroma lamellae

Introduction

In plants and algae, multiple reactions catalyze light-driven electron transport from water to $NADP^+$, sustain ATP production, and lead to CO_2 fixation into organic compounds. The photosynthetic machinery includes the thylakoid membrane supercomplexes Photosystems (PS) II and I, which are functionally connected by the electron carrier plastoquinone (PQ), cytochrome b_6f complex, and plastocyanin. Chlorophylls (Chl) and carotenoids (Car), chromophores binding to each PS, ensure photon absorption and rapid transfer of the excitation energy to the reaction center (RC), fueling charge separation (Nelson and Ben Shem 2004).

PSI catalyzes electron transport from plastocyanin to ferredoxin. PSI core binds Chl *a*, β-carotene, and all the co-factors required for electron transport (Qin et al. 2015; Mazor et al. 2015). Also, a peripheral antenna system (LHCI, light-harvesting complex of PSI) enlarges the PSI absorption cross-section. LHCI, in *Arabidopsis thaliana*, consists of 4 light-harvesting proteins (Lhca1–Lhca4), encoded by single genes (Jansson 1999), that bind Chl *a*, Chl *b*, xanthophylls, and β-carotenes (Qin et al. 2015; Mazor et al. 2015). Despite the fact that Lhcas share similarities in structure and pigment organization with members of the LHC family (Liu et al. 2004; Amunts et al. 2010; Pan et al. 2011; Qin et al. 2015), these antennae display peculiar spectroscopic properties, including "red spectral forms", which

Deletion of the LHCI antenna system of Photosystem I impairs relocation of the mobile LHCII pool between thylakoid domains upon state transitions.

Electronic supplementary material The online version of this article (doi:10.1007/s11120-017-0444-1) contains supplementary material, which is available to authorized users.

✉ Roberto Bassi
roberto.bassi@univr.it

[1] Dipartimento di Biotecnologie, Università di Verona, Strada Le Grazie 15, 37134 Verona, Italy

Published online: 16 September 2017

originate from Chl with energies lower than P700 RC (Lam et al. 1984).

However, the high conservation of LHCI subunits suggests a specific function for LHCI in the acclimation to environmental cues. Indeed, characterization of *Arabidopsis* mutants with decreased levels of Lhcas (Klimmek et al. 2005) showed a reduced fitness under natural conditions (Ganeteg et al. 2004).

A peculiar property of the peripheral antenna system is its ability to modulate the light-harvesting capacity of PSs and to optimize electron transport in response to the light environment (Horton et al. 1996; Dall'Osto et al. 2015), namely the fluctuations in both intensity and spectrum, which easily yield into unbalanced excitation of PSs and decrease the photosynthetic efficiency (Pesaresi et al. 2010). PSII and PSI regulate light harvesting differently: PSII typically displays (i) a short-term feed-back control of excess excitation energy (Ruban et al. 2012) and (ii) a long-term decrease in LHCII content under excess light. Instead, neither the light-harvesting efficiency of LHCI nor the PSI core/LHCI ratios were affected by sustained over-excitation (Anderson 1986; Ballottari et al. 2007; Cazzaniga et al. 2016). Rather, the PSII/PSI excitation imbalance is compensated by recruiting LHCII as a supplementary antenna for PSI through the mechanism of state transitions (ST) (Allen 1992; Galka et al. 2012). ST reorganize the PSs antenna system on a timescale of minutes, and involve the relocation of a mobile LHCII pool, which reversibly associates with either PSI or PSII. PSII over-excitation reduces PQ to PQH_2 which activates thylakoid protein kinase STN7 and, in turn, phosphorylates LHCII (Bellafiore et al. 2005). These reactions ultimately yield into the so-called state II, with enhanced PSI antenna size and electron transport activity. Conversely, over-excitation of PSI results in oxidation of the PQ pool, inactivation of the LHCII kinase, and dephosphorylation of P-LHCII by TAP38 phosphatase (Pribil et al. 2010). De-phosphorylated LHCII detaches from PSI and return to PSII (state I).

While ST involve LHCII, recent results (Benson et al. 2015) showed that the absence of specific Lhca subunits reduces amplitude of ST in *Arabidopsis*, with *ΔLhca4* plants showing the most severe phenotype. On the other hand, Bressan et al. (2016) reported that energy transfer efficiency from LHCII to PSI was, if any, slightly increased in the absence of LHCI, meaning that LHCII is a very good antenna for PSI, with or without its LHCI moiety. Here, we analyze in detail the mechanism of ST in the absence of LHCI system. To this aim, we used the *Arabidopsis ΔLhca* mutant, devoid of all Lhca1-4 subunits (Bressan et al. 2016), and studied its response to changes in light quality. Due to a smaller PSI antenna size, PQ pool of *ΔLhca* plants was more reduced than in the wild type even under conditions promoting the formation of PSI–LHCII supercomplexes (Bressan et al. 2016) and, consistently, LHCII binding to PSI was greatly increased. Instead, decrease of Fm, commonly observed upon state I-state II transition, was strongly reduced in the mutant, suggesting that LHCII fluorescence quenching by PSI was impaired. We observed that lateral heterogeneity of thylakoids membranes, and distribution of LHCII between thylakoid domains was affected in the mutant with respect to the wild type, which might explain the decreased amplitude of fluorescence changes upon ST.

Materials and methods

Plant material and growth conditions

The *Arabidopsis thaliana ΔLhca* mutant was obtained as reported in Bressan et al. (2016). Plants were maintained in a growth chamber for 5 weeks at 150 µmol photons m^{-2} s^{-1} (OSRAM halogen HQI-T 250W and/or OSRAM lumilux cool white L58W), 23 °C, 70% humidity, and 8/16 h of day/night. Induction of either state I or state II was obtained by illuminating plants for 45 min with a PSI light (30-W incandescent bulbs filtered through Lee Filters 027 Medium Red) or a PSII light (30-W warm white fluorescent lamps filtered through Lee Filters 105 Orange), respectively, according to Pesaresi et al. (2009).

Membrane isolation

Stacked thylakoid membranes were isolated as in Casazza et al. (2001). Grana-, margin-, and stroma-enriched fractions were isolated as in Barbato et al. (2000).

Pigment analysis

Pigments were extracted from leaf disks with 85% acetone buffered with Na_2CO_3, separated and quantified by HPLC (Gilmore and Yamamoto 1991).

Spectroscopy

Absorption measurements were performed using a SLM Aminco DW-2000 spectrophotometer at RT either on samples in 10 mM HEPES pH 7.5, 20% (w/v) glycerol, 0.05% α-DM or 0.05% digitonin, or directly on leaves. Fluorescence emission spectra were measured at RT using a Jobin–Yvon Fluoromax-3 spectrofluorimeter.

Gel electrophoresis, immunoblotting, and sample preparation

SDS-PAGE analysis was performed with the Tris–Glycine buffer system (Laemmli 1970) with some modifications (Ballottari et al. 2004), and the Tris–Tricine buffer

system (Schägger and von Jagow 1987). Non-denaturing Deriphat-PAGE and CN-PAGE were performed following the methods described by Peter et al. (1991) and Jarvi et al. (2011). Thylakoids brought to 1 mg/mL Chls were solubilized in 0.1% α-DM and 0.5% digitonin (Galka et al. 2012). After electrophoresis, bands corresponding to PSI supercomplexes were excised, ground in extraction buffer (0.02% digitonin, 30% glycerol, 10 mM Hepes pH 7.5), and then further purified by ultracentrifugation (Galka et al. 2012). For immunotitration, membrane protein samples were fractionated by SDS-PAGE, electroblotted onto nitrocellulose membranes, and proteins were detected using specific primary antibodies: α-Lhcb1/2/3 (AS01 004/003/002), α-PsaA (AS06 172), α-PsbB (AS04 038), and α-P-Lhcb1 (AS13 2704) from Agrisera. The alkaline phosphatase-conjugated secondary antibody was purchased from Sigma-Aldrich (A3687).

Cross-linking was carried out as described in Jansson et al. (1996): purified PSI–LHCI–LHCII and PSI–LHCII complexes (0.05 nmol complex/μL in 10 mM Hepes pH 7.5, 0.1% digitonin) were cross-linked with DTSP (final concentration 0.015%) at RT for 30 min. Samples were solubilized in a non-reducing sample buffer and electrophoresed on 10–20% polyacrylamide gels (Tris–Glycine buffer system). The lanes were cut out and incubated for 30 min in a sample buffer containing 50 mM DTT + 5% β-mercaptoethanol to cleave the cross-links. The gel slice was placed on top of a second 8–25% polyacrylamide gel and re-electrophoresed. Both α-P-Lhcb2-conjugates (Agrisera AS13 2705) and α-PsaH-conjugates (Agrisera AS06 105) were detected.

Analysis of Chl fluorescence

State transitions were measured on whole leaves at RT with a PAM 101 fluorimeter (Heinz-Walz) according to Jensen et al. (2000). Minimum fluorescence (F_0) was measured with a 0.15 μmol photons m^{-2} s^{-1} beam, and maximum fluorescence (F_m) was determined with a 0.8-s light pulse (4500 μmol photons m^{-2} s^{-1}, supplied by a KL1500 halogen lamp, Schott). Preferential PSII excitation was provided by illumination with white actinic light filtered through Lee Filters 105 Orange (Pesaresi et al. 2009) at an intensity of 50 μmol photons m^{-2} s^{-1}, while excitation of PSI was achieved using far-red light from an LED light source (Heinz-Walz, 102-FR) applied simultaneously with orange light. F_s is the stationary fluorescence during illumination. F_m levels in state I (F_m') and state II (F_m'') were determined at the end of each actinic cycle by applying a saturating light pulse. The parameter qT (PSII cross-section changes) was calculated as $(F_m' - F_m'')/F_m' \times 100$.

Electron microscopy

Intact leaf fragments from wild type and mutant 5-week-old plants, grown under controlled conditions, were fixed, embedded, and observed in thin section (de Bianchi et al. 2008).

Results

ΔLhca is a knock-out mutant of Arabidopsis, devoid of the PSI peripheral antenna system

ΔLhca plants (Bressan et al. 2016), grown in a climate chamber (150 μmol photons m^{-2} s^{-1}, 23 °C, 8/16 day/night) for 5 weeks, were significantly smaller than wild type (Fig. 1a). The organization of pigment-binding supercomplexes was analyzed by non-denaturing Deriphat-PAGE, after solubilizing wild-type and *ΔLhca* thylakoids in 0.6% α-DM (Fig. 1b). Several green bands were resolved: in both wild type and mutant, the PSII pigment–proteins migrated as multiple bands with different apparent masses, i.e., the PSII dimeric core and the PSII supercomplexes of different LHCII compositions. No significant differences were observed in both mobility and relative abundance of PSII bands in thylakoids from wild type and *ΔLhca*. The PSI-LHCI supercomplex was present as a single major band in the wild type, co-migrating with PSII dimeric core. The most evident difference detected in *ΔLhca* versus wild type was the lack of PSI-LHCI supercomplex and the presence of a green band with lower apparent mass, corresponding to the core moiety of PSI (Bressan et al. 2016). As revealed by immunoblotting (Fig. 1c), the *ΔLhca* mutant was devoid of all four Lhca subunits.

Regulation of PSI antenna size upon state I–state II transitions

The stunted growth of *ΔLhca* plants (Fig. 1a) could be ascribed to an imbalance in the distribution of excitation energy between the two PSs, as a consequence of LHCI depletion and reduced optical cross-section of PSI. Optimization of linear electron transport is normally ensured by rapid relocation of LHCII between PSs through the process of state I–state II transitions: over-reduction of the PQ pool promotes LHCII phosphorylation, which causes the displacement of LHCII from PSII to PSI (state II); in contrast, an enhanced excitation of PSI oxidizes the PQ pool and reverses the process to state I.

To investigate whether the lack of LHCI affected photosynthetic electron flow under different light quality, the ST activity was measured on leaves as changes in Chl fluorescence upon PQ reduction (Jensen et al. 2000) (Fig. 2a).

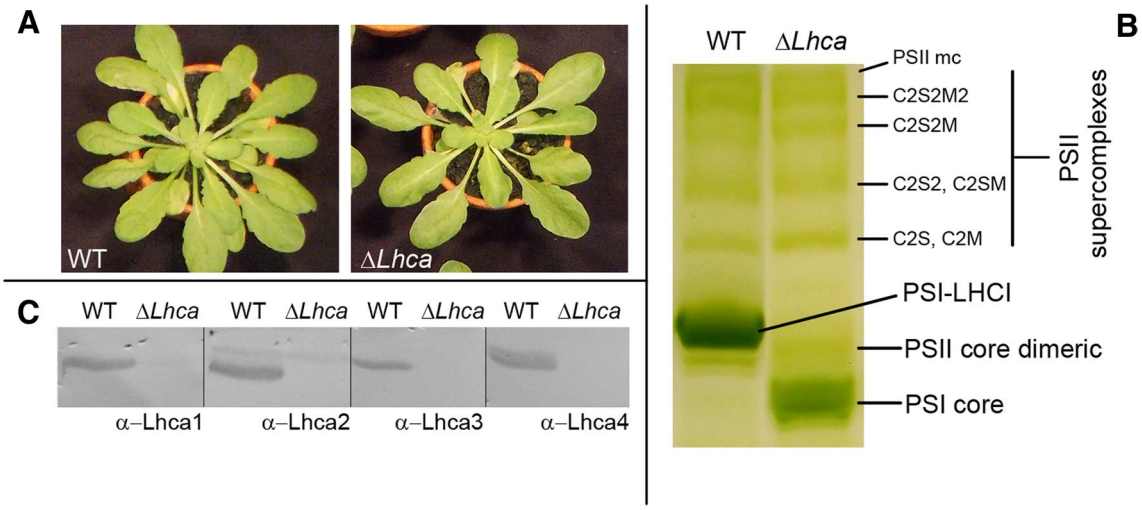

Fig. 1 Characterization of *koLhca* mutant line. **a** Phenotype of wild-type and mutant plants, grown in soil for 5 weeks under controlled conditions (150 µmol photons m^{-2} s^{-1}, 23 °C, 8/16 h day/night regime). **b** Thylakoid pigment-protein complexes were separated by non-denaturing Deriphat-PAGE upon solubilization with 0.6% α-DM. Thylakoids corresponding to 25 µg of Chls were loaded in each lane. The major pigment-protein complexes are indicated; nomenclature of PSII supercomplexes as in Caffarri et al., EMBO J. 2009. PSII mc, PSII megacomplexes. **c** Western-blot analysis of leaf extracts, with antibodies specific for the proteins indicated in each filter

The fluorescence pattern of *ΔLhca* differed in many respects from that of the wild type and, in particular, the steady-state fluorescence level in light-adapted leaves (F_s) was far higher in *ΔLhca* during illumination with orange light. Upon addition of 725 nm far-red (FR) light, a marked decrease in fluorescence was observed in both genotypes, consistent with the oxidation of the PQ pool. When the FR light was switched off, both genotypes displayed a similar increase in fluorescence, brought about by the reduction of the PQ pool, followed by a decay whose amplitude was far smaller in *ΔLhca* than the wild type, leading to a greatly reduced qT value (see "Materials and methods") in *ΔLhca* (1.1 ± 0.3) with respect to wild type (8.4 ± 0.1). Thus, despite F_s/F_o being higher, consistent with a chronically higher reduction level of PQ, the apparent amplitude of ST was lower in *ΔLhca* than in wild-type plants.

We checked the phosphorylation state of both Lhcb1 and Lhcb2 by immunoblotting with specific antibodies after a 45-min exposure of the plants to either PSI or PSII light (Supplemental Figure S1). In state I, no LHCII phosphorylation was detected in either the wild type or *ΔLhca*. In state II, P-LHCII was detected in both and yet, while the level of P-Lhcb1 was similar in both genotypes, P-Lhcb2 was far more abundant (+75%) in the *ΔLhca* mutant, thus implying that the decreased amplitude of ST in *ΔLhca* was neither due to an altered activity of the kinase STN7 nor due to a reduced level of the mobile LHCII subpopulation (Leoni et al. 2013). We investigated the ability of *ΔLhca* to form PSI–LHCII supercomplexes by non-denaturing CN-PAGE of thylakoid samples, adapted to either state I or state II and solubilized by digitonin (Fig. 2b). Exposure to PSII light led to the formation of new PSI-containing green bands with higher MW in both the wild type and *ΔLhca*, which were absent in samples harvested from state I-adapted leaves. These high MW bands were consistent with the formation of LHCII-binding PSI supercomplexes. In *ΔLhca*, the PSI–LHCII band was three times more abundant than the corresponding PSI-LHCI-LHCII band found in the wild-type sample under the same conditions (Fig. 2b). These pigment-protein bands were eluted from the gel matrix and characterized. Absorption spectra (Fig. 2c) were normalized based on Chl molar concentration (Galka et al. 2012) and Chl to protein stoichiometry (Liu et al. 2004; Qin et al. 2015) and the difference spectra were calculated, namely (PSI-LHCI-LHCII *minus* PSI-LHCI) from wild-type samples and (PSI–LHCII *minus* PSI core) from *ΔLhca*. In both cases, a typical trimeric LHCII spectrum was obtained while the amplitude was consistent with a single LHCII trimer per PSI. To determine whether the interaction mode between PSI and LHCII was the same in the presence or absence of LHCI, the LHCII-containing complexes were subjected to chemical cross-linking with DTSP and analyzed by diagonal electrophoresis. The final 2D map was probed with anti-PsaH, a subunit involved in the association of the mobile pool of LHCII to PSI (Zhang and Scheller 2004; Crepin and Caffarri 2015) and with anti-P-Lhcb2 (phosphorylated-Lhcb2). The pattern of cross-linked products was essentially the same for both samples (Supplemental Figure S2), suggesting that the site of LHCII interaction with PSI was the same in both supercomplexes.

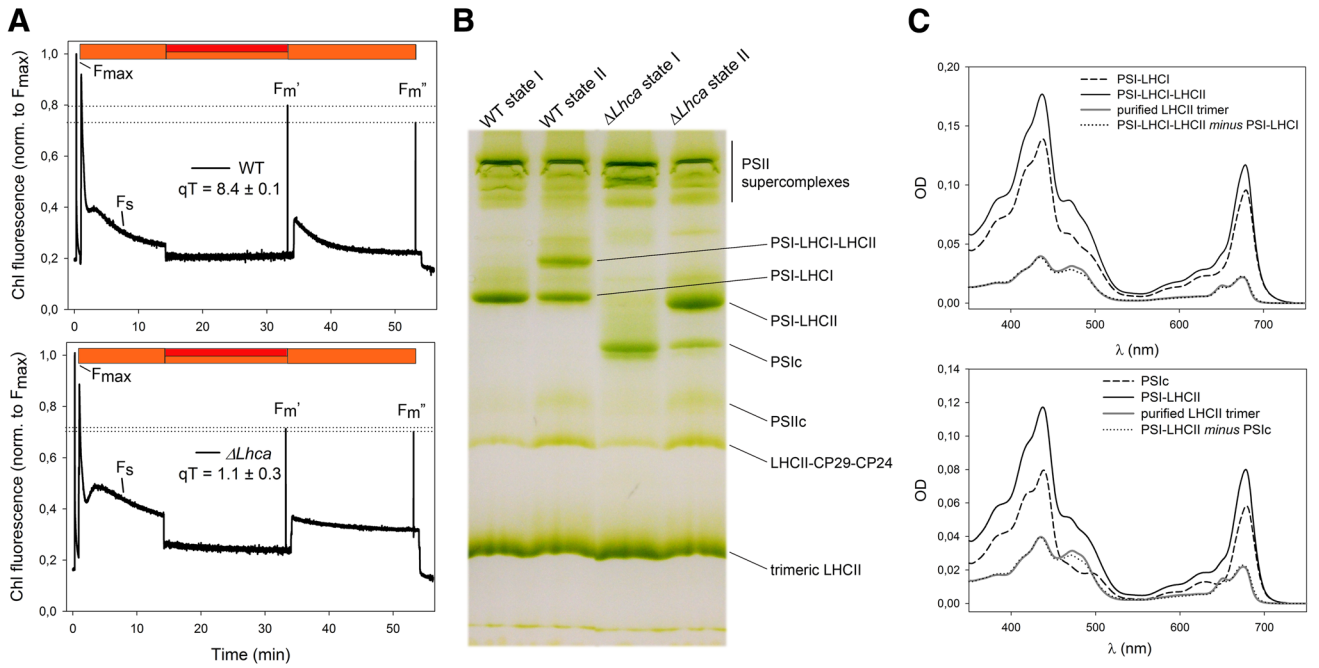

Fig. 2 Measurement of state I–state II transitions and identification of the PSI-LHCI-LHCII complex. **a** Dark-adapted wild-type (upper panel) and mutant (lower panel) leaves were illuminated with orange light (50 µmol photons m^{-2} s^{-1}, Lee Filters 105 Orange, see "Materials and methods" section) for 15 min to reach state II, then a far-red light (PAM lamp FR-105) was superimposed on the orange one to induce a transition to state I. Values of F_m, F_m', and F_m'' were determined using light saturation pulses. Amplitudes of state transitions (parameter qT, reported as mean ± SD, $n = 3$) were determined as reported in Methods. qT values are significantly different between the two genotypes (Student's t test, $P < 0.05$, $n = 3$) (**b**) CN-PAGE of thylakoid proteins isolated from wild-type and *ΔLhca* plants acclimated either to PSI or PSII light for 45 min before membrane isolation. A PSI-LHCI-LHCII supercomplex is only visible in wild-type leaves treated with PSII light, whereas in the corresponding mutant sample, a complex with higher apparent mass than that of the PSI core represents the PSI–LHCII supercomplex. These complexes are absent in the leaves treated with PSI light. **c** Absorption spectra of PSI-LHCI and PSI-LHCI-LHCII purified from wild-type plants (upper panel), and of the PSI core and PSI–LHCII purified from *ΔLhca* ones (lower panel), normalized to the same molar concentration: on the basis of their Chl contents, ratios of peaks in the Q_y absorption band, of complexes at the same molar concentration, were calculated; once normalized the absorptions of supercomplexes by this ratio, and determined the difference spectra, we found that they were very similar to that of a trimeric LHCII. For each genotype, the difference spectrum is compared with the spectrum of a purified trimeric LHCII. PSIc/PSIIc, PSI/PSII core complex

Distribution of LHCII among thylakoid domains upon state I–state II transitions

Biochemical analysis indicated a stronger increase in PSI antenna size in *ΔLhca* versus wild type, inconsistent with the RT Chl fluorescence analysis (Fig. 2a). In order to elucidate the origin of this discrepancy, we proceeded to the characterization of thylakoid lateral heterogeneity in the two genotypes. EM analysis showed that wild-type thylakoids had the typical organization with grana stacks interconnected by stroma membranes, while the mutant plants had grana partitions but with larger diameter, as determined by the number of thylakoids per granum and the length of paired grana partitions and stroma lamellae (Fig. 3; Table 1). Fractionation of the membranes in grana, margin, and stroma lamellae by treatment with digitonin (Barbato et al. 2000), and quantification of Chl distribution between the different domains, was consistent with EM analysis: in state I, yield of grana-enriched membrane was significantly lower in mutant plants (−20%), while yield of stroma fractions was 31% higher in *ΔLhca* versus wild type (Table 2).

To gain additional insights on the effect of ST on the quenching capacity of LHCII by PSI, we then proceeded to evaluate changes in fluorescence from whole thylakoids and the purified domains, measured at RT (Fig. 4, upper panels). Transition to state II led to a decrease of fluorescence yield per unit Chl of thylakoids in both genotypes. However, the difference was significantly higher in wild-type sample (−36 ± 8%) than in the mutant (−10 ± 4%) (Fig. 4a). In both wild type and *ΔLhca*, grana showed the highest fluorescence yield, followed by margins and, far lower, by stroma lamellae (Fig. 4b). This suggests that the contribution of stroma membranes to the overall fluorescence yield of thylakoids was indeed limited, consistent with PSII in grana fractions being the major source of fluorescence at RT. Transition to state II decreased fluorescence yield of both grana and margins in wild type, consistent with the loss of LHCII caused by migration

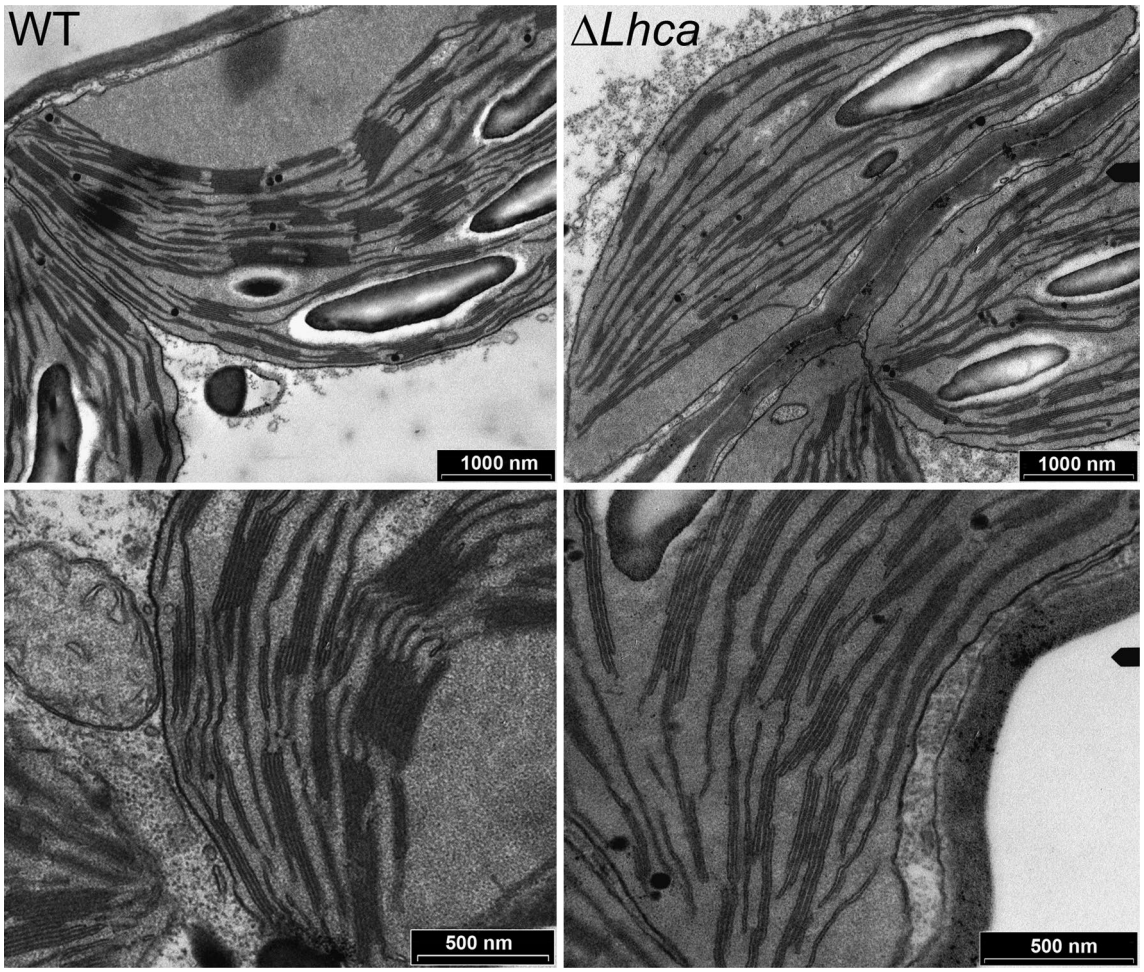

Fig. 3 Transmission electron micrographs of plastids from mesophyll cells of the wild type and *ΔLhca*. Plants grown in short-day conditions were dark-adapted for 6 h before harvesting leaves, then samples were fixed, embedded, and observed in thin section at two different levels of magnification. Wild type, left panels; *ΔLhca*, right panels. In both genotypes, chloroplasts showed a characteristic organization of stroma lamellae and interconnecting grana stacks. However, statistical analysis (see Table 1) revealed that the mutant plastids had a lower number of grana partitions but with larger diameter than the wild type

Table 1 Statistical analysis of differences in chloroplast ultrastructure in wild type and mutant

	WT	*ΔLhca*
Grana per chloroplast[a]	31.3 ± 1.4	38.4 ± 6.1*
Stacks per granum[b]	6.9 ± 2.4	4.9 ± 1.9*
Diameter of grana (μm)[b]	0.50 ± 0.08	0.76 ± 0.20*
Length of stroma lamellae (μm)[b]	0.35 ± 0.12	0.69 ± 0.22*

Data are expressed as means ± SD ([a]$n = 10$ or [b]$n > 40$). Values that are significantly different (Student's t test, $P < 0.05$) from the wild type are marked with an asterisk (*)

Table 2 Chl distribution between different thylakoid domains in wild type and *ΔLhca*

	Mol Chl (%)		
	Grana	Margins	Stroma fractions
WT state I	47 ± 4[a]	24 ± 3[a]	29 ± 4[a]
WT state II	34 ± 5[b]	29 ± 1[b]	37 ± 5[b]
ΔLhca state I	38 ± 3[b]	24 ± 2[a]	38 ± 3[b]
ΔLhca state II	38 ± 4[b]	25 ± 3[a]	37 ± 4[b]

Upon treatment with digitonin and differential centrifugation, we quantified the distribution of Chl into different domains as a measure of the yield. Values are reported as mean of 2 independent preparations. Values that are significantly different within the same column (Student's t test, $P < 0.05$, $n = 4$) are marked with different letters

of LHCII towards the margin and stroma regions in state II and efficient quenching in these domains; emission of stroma membranes was increased upon ST, although to a different extent (+ 49% in wild type, +7% in *ΔLhca*) (Fig. 4b). In contrast, fluorescence yield of all thylakoid

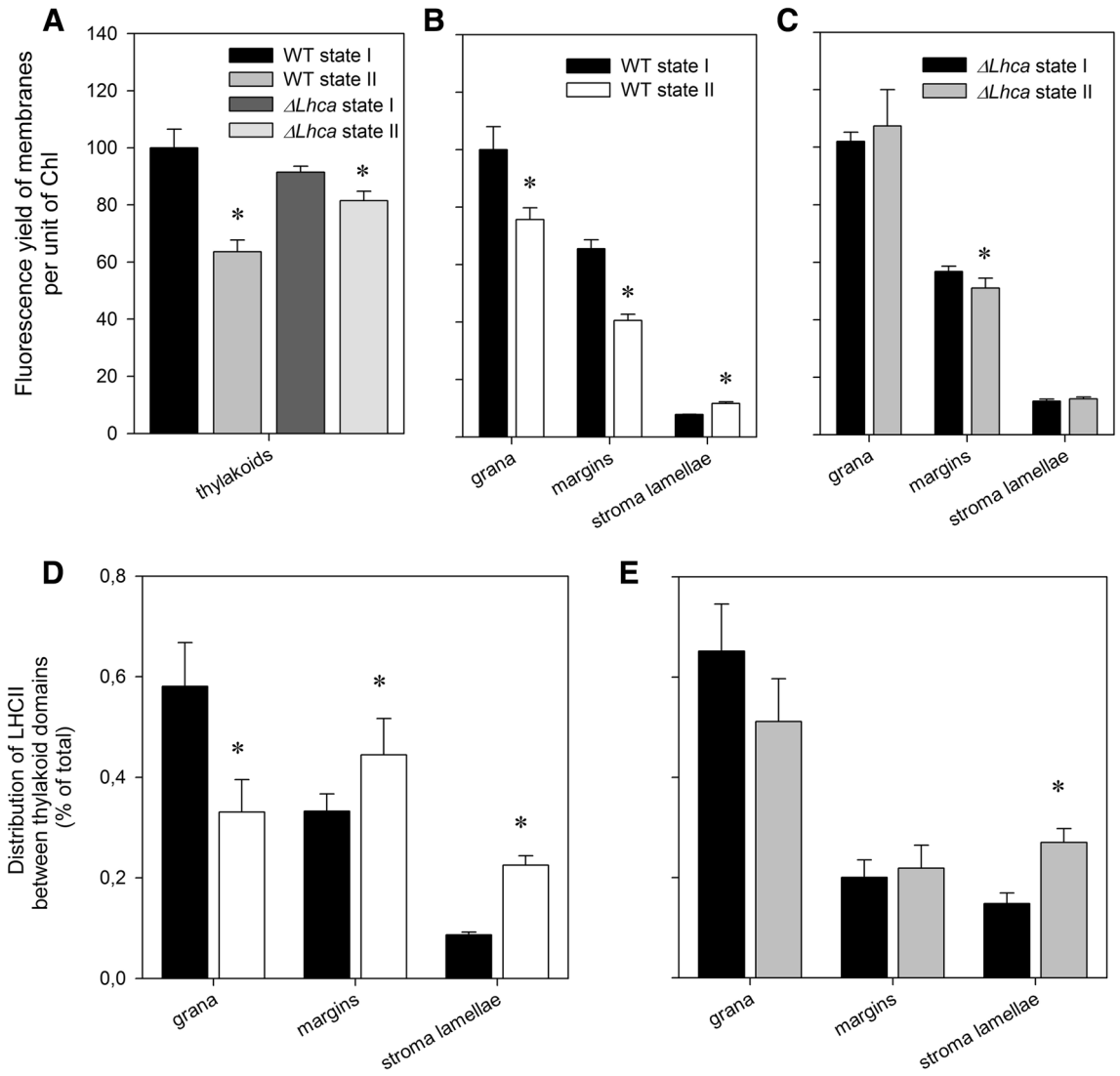

Fig. 4 Effect of altered lateral heterogeneity on RT fluorescence analysis of state transitions. **a–c** Grana, margins, and stroma lamellae were isolated with digitonin solubilization of thylakoids either in state I or state II, analyzed by SDS-PAGE (see Supplemental Figure S3), then fluorescence emission yield of whole thylakoids (panel **a**) and thylakoid domains (panel **b, c**) were determined. Spectra were recorded at RT, $\lambda_{exc} = 475$ nm, $\lambda_{ems} = 680$ nm. Samples were diluted to the same Chl concentration (0.2 µg/mL). GFP (1 µM) was added to the membranes suspension as an internal standard. Each measure is the average of 4 records. Fluorescence yields were normalized to that of wild-type thylakoids in state I (panel **a**), to that of grana in state I (panel **b, c**). **d, e** Quantitative analysis of LHCII distribution between thylakoid fractions was carried out by SDS-PAGE and immunotitration analysis. Results are representative of two independent procedures of thylakoids isolation and solubilization. Significantly different values, within the same domain, are marked with an asterisk (Student's *t* test, $P < 0.05$, $n = 3$)

domains from *ΔLhca* was far less affected by state II induction (Fig. 4c).

Re-distribution of LHCII between the different domains is likely the major determinant in such fluorescence changes; thus, we quantified the lateral distribution of the major antenna upon ST, by SDS-PAGE (Supplemental Figure S3). In wild type, as a consequence of state II induction, a decrease in the LHCII content was observed in grana membranes (−25.1% of total LHCII), while a fraction of LHCII migrated to margin (11.2%) and stroma regions (13.9%) (Fig. 4c). Such a migration of LHCII is consistent with the observed decrease in fluorescence yield of the grana domain and with an effective quenching of LHCII fluorescence in both margins and stroma domains (Fig. 4b).

LHCII was more abundant in the stroma membranes of the mutant (14.8 ± 2.1% of total LHCII) versus wild type (8.6 ± 0.6%) already in state I, and further increased upon ST (Fig. 4d). The enrichment in LHCII was significantly smaller in the mutant (+ 82 ± 26%) than in wild-type membranes (+ 160 ± 27%). Moreover, a lower fraction of LHCII (1.8%

of total LHCII in *ΔLhca* versus11.1% in wild type) migrated from grana partitions to margin domains upon ST.

Analysis of re-distribution of PSI core complex in the different domains revealed it was essentially unaffected in both genotypes; PSII core relative abundance, instead, increased in margin domains upon ST in the wild type only (Supplemental Table S1). Increased LHCII content did enhance fluorescence yield of stroma membranes and yet this was evident in wild type only, while stroma membranes fraction from *ΔLhca* maintained the same fluorescence yield despite increased LHCII content (Fig. 4b, c).

Treatment with α-DM to 0.05% allowed for normalization to LHCII content, whose fluorescence yield was dominant in detergent conditions (Supplemental Figure S4), thus revealing the effect of phosphorylation in promoting LHCII quenching by PSI. In both genotypes, normalized fluorescence yield was higher in state I versus state II, implying that phosphorylation was necessary for fully efficient LHCII quenching by PSI. However, the difference in yield was far higher in stroma lamellae from wild type with respect to *ΔLhca*, suggesting a limited capacity for LHCII quenching by PSI in isolated stroma membranes.

Discussion

In *ΔLhca* plants, the knocking out of three of the four *Lhca* genes, encoding LHCI subunits, caused the deletion of the entire PSI peripheral antenna system. Lack of LHCI could not be compensated by binding other LHC gene products within Lhca-binding sites (Bressan et al. 2016). These results confirm that PSI-LHCI is a stable system (Klimmek et al. 2005; Ballottari et al. 2007), lacking the plasticity in the composition of outer antenna typical of PSII (Ruban et al. 2003). We thus analyzed the effect of LHCI depletion on the plant ability to respond to light conditions which preferentially stimulate one or the other of the PSs. In *ΔLhca* plants, the reduced absorption cross-section of PSI affected its capacity for maintaining redox balance. A compensatory mechanism increased the levels of PSI–LHCII$_{n=1}$ supercomplexes (digitonin-insensitive) with respect to the wild type (Fig. 2b). Nevertheless, a single LHCII trimer (42 Chls) could not fully compensate for the missing LHCI (57 Chls) (Liu et al. 2004; Qin et al. 2015; Bressan et al. 2016). Therefore, despite greatly enhancing the formation of PSI–LHCII supercomplexes, the mutant was unable to restore a normal growth rate in limiting light.

Contrasting biochemical versus fluorescence ST phenotype

The *ΔLhca* mutant exhibited an intriguing ST phenotype. Its PQ pool was more reduced than that of the wild type and the capacity for ST in terms of formation of PSI–LHCII$_{n=1}$ supercomplexes was strongly enhanced, as consistently shown by biochemical measurements (Fig. 2b). However, F_m changes upon switching off far-red light (Fig. 2a) suggested a reduced capacity for LHCII fluorescence quenching by PSI in the mutant. Based on recent report (Bressan et al. 2016), excitation transfer efficiency from LHCII to PSI in the absence of LHCI was slightly increased, rather than impaired. LHCII, thus, is a good antenna for the PSI complex irrespective of being endowed with LHCI or not, and this makes the biochemical phenotype in contrast with the RT fluorescence phenotype. To understand the reasons for discrepancy, we considered the possibility that the lack of LHCI could affect the lateral heterogeneity of thylakoids membranes. Indeed, an altered distribution of LHCII, namely the thylakoid pigment-protein complex with the highest fluorescence yield (Engelmann et al. 2005), between grana and stroma lamellae, could well affect the overall fluorescence yield of thylakoids. The mutant had (i) a higher ratio of stroma membranes to grana stacks, and (ii) grana membranes with a lower number of partitions than the wild type (Fig. 4; Table 1). Induction of ST decreased fluorescence yield of thylakoids in both genotypes, although the change was far higher in wild-type sample (Fig. 4a). Upon analyzing specifically grana, margins and stroma lamellae, we found that in wild-type transition to state II led to a significant decrease in fluorescence yield of both grana and margins per unit of Chl, while stroma lamellae increased their fluorescence yield (Fig. 4b). Decreased fluorescence yield correlated with a migration of P-LHCII towards margins and stroma lamellae (Fig. 4d), where it was efficiently quenched, likely by PSI (Supplemental Figure S4) (Galka et al. 2012). In *ΔLhca*, instead, the fluorescence changes induced by state transition were minimal. Thus, the reduced ST phenotype in *ΔLhca* (Fig. 2a) was due to events occurring in grana and margin domains rather than in stroma membranes. It is relevant to discuss the relation between LHCII content and fluorescence yield in thylakoid domains, whose composition and the changes induced by state I–state II transition can be measured by SDS-PAGE analysis (Liu et al. 2004; Qin et al. 2015) and by quantification of Chl distribution between thylakoid domains (Supplemental Figure S3, Table 2). In wild-type stroma membranes, the stoichiometry of trimeric LHCII per PSI core increased from 0.81 ± 0.07 in state I to 1.85 ± 0.15 in state II. In the mutant, stromal lamellae contained more LHCII in state I already (1.65 ± 0.08 trimers/PSI), further enhanced to 3.22 ± 0.45 in state II. This LHCII pool was efficiently quenched, likely by PSI (Supplemental Figure S4). Clearly, phosphorylation was needed for optimal quenching of LHCII fluorescence since the stroma lamellae from wild type decreased their fluorescence yield (normalized to LHCII content) in state II versus state I despite the doubling in LHCII content (Supplemental

Figure S4, Fig. 4d). However, the fluorescence yield of the unsolubilized stroma membranes increased upon addition of LHCII in wild type but not in *ΔLhca*, despite the increase in LHCII content was similar. In order to explain this contradiction, we note that low fluorescence yield in stroma lamellae was observed in samples with LHCII/PSI ratio below unity, while higher than 1 ratios produced the same fluorescence yield (wild-type state II, *ΔLhca state I, state II)*. These findings suggest that stroma membranes have two distinct mechanisms for quenching LHCII complexes: the first depends on phosphorylation and occurs at PSI:LHCII stoichiometry below 1, the second occurs at PSI/LHCII stoichiometry higher than 1 and is independent of phosphorylation (Supplemental Figure S4). The underlying mechanism is unclear but could involve aggregation of LHCII in excess with respect to PSI (Dall'Osto et al. 2014; Unlu et al. 2014).

Although interesting, changes in fluorescence yield of stroma membranes cannot account for the relevant fluorescence changes of either isolated thylakoid (Fig. 4a) or in vivo (Fig. 2a) due to their low contribution to fluorescence emission (Fig. 4b, c). It is thus relevant to discuss changes in the yield of highly fluorescent compartments: grana and margins. In wild type, LHCII content of margins in state I was higher in wild type (35% of total LHCII localizes in this domain) with respect to the mutant (20% of total LHCII in margins). Moreover, LHCII content of margins (i) increased upon ST, and (ii) was efficiently quenched in state II with respect to state I (Fig. 4b). This result is consistent with the previous reports (Tikkanen et al. 2008; Benson et al. 2015) showing that PSI cross-section increased preferentially in margins upon ST. In *ΔLhca*, instead, ST did not affect neither LHCII content nor fluorescence yield of margins, suggesting an impairment in both LHCII migration out of grana partitions and in LHCII quenching mechanisms active in the margins of wild-type plants.

It can thus be concluded that the overall decrease in F_m exhibited by wild type upon ST correlates with an increased LHCII content in margin and stromal domains, and decreased LHCII/PSII ratio in grana. This is likely due to the shorter lifetime of PSII core complexes with respect to LHCII (Engelmann et al. 2005). LHCII migration out of grana partitions did occur to a reduced extent in the case of *ΔLhca*, despite the increase in LHCB2 phosphorylation (Supplemental Figure S1), thus minimizing the F_m decrease upon transition to state II (Fig. 2a).

LHCII migration between thylakoid domains is impaired in ΔLhca

It is relevant to discuss the reasons for the decreased efficiency of LHCII migration out of grana partitions in *ΔLhca*. One possibility is that the increased grana size in mutant versus wild type (Fig. 3) limits the interface between these domains through which diffusion occurs. Also, the over-reduction state of PQ in *ΔLhca* might cause an enrichment of Lhcb2 in stoma membranes: during state II-inducing treatment, Lhcb2 would be more exposed to STN7 activity, also located in stroma (Pesaresi et al. 2011; Betterle et al. 2015) yielding into high phosphorylation but reduced migration. However, analysis of Lhcb1-3 relative content in stroma lamellae revealed no significant changes in both genotypes upon ST induction (Supplemental Figure S5), inconsistent with this hypothesis.

Alternatively, the large decrease of LHCII content in wild-type grana could be in part ascribed to the remodeling of thylakoid assembly upon ST. Chuartzman et al. (2008) recently showed that, consequent to LHCII migration from the grana to the stroma lamellae, margins of the granum body became unstable and adjacent layers retracted from each other, leading to unstacking and partial disassembly. Consistently, we found that solubilization of wild-type state II thylakoids resulted in a significantly lower yield in grana membranes with respect to state I, while a corresponding increase in the yield of stroma lamellae was observed (Table 2). Thus, the reduction of LHCII content measured in wild-type grana could be somehow over-estimated by the structural rearrangements in the granum–stroma interface domain upon ST. However, it is worth noting that (i) the Chl distribution between thylakoid domains was unaffected by ST in *ΔLhca* (Table 2), and (ii) the re-distribution of LHCII was reduced in the mutant (Fig. 4d, e). This supports the idea that lateral movement of LHCII between thylakoid domains is impaired in the absence of LHCI.

A further possibility is that lack of LHCI could impair LHCII association to PSI. A number of studies indicate that multiple LHCIIs can bind to PSI in plants (Benson et al. 2015; Bell et al. 2015; Yadav et al. 2017), while LHCIIs increased the absorption cross-section of PSI (Bos et al. 2017). The digitonin-insensitive fraction of trimers was connected to PSI near the PsaH subunit (Lunde et al. 2000; Galka et al. 2012). Instead, the fraction which dissociates in the presence of digitonin likely represents the LHCIIs that are coupled to the LHCI side of the PSI–$LHCII_{n>1}$ complex. Indeed, Benson et al. (2015), showed that a subpopulation of PSI and LHCII energetically interacts through LHCI in margins, and with the identification of PSI–$LHCII_2$ particles, with one LHCII at the PsaH side and a second one close to Lhca2 by EM (Yadav et al. 2017).

Based on antenna size measurements (Benson et al. 2015), it has been proposed that all PSI in the margins are associated with at least one LHCII trimer in wild-type state II thylakoids, while deeper in the stromal domains only a fraction of PSI coordinates LHCII complexes.

In *ΔLhca* plants, the reduced absorption cross-section of PSI might be exacerbated by the impaired formation of PSI–$LHCII_{n>1}$ supercomplexes, thus up-regulating a

compensatory mechanism which increases the levels of PSI–LHCII$_{n=1}$ supercomplexes (digitonin-insensitive) in stroma lamellae with respect to the wild type (Fig. 2).

In *A. thaliana*, both LHCII-S and LHCII-M trimers are thought not to be involved in ST (Galka et al. 2012; Bos et al. 2017) while the mobile antenna involves the so-called "extra LHCIIs." The model of state transitions predicts that LHCII phosphorylation triggers its dissociation from PSII and its migration to PSI. However, in mutants devoid of either PSI (Delosme et al. 1996) or PsaH-binding site for LHCII (Lunde et al. 2000), docking is impaired and P-LHCII is retained in the grana, thus suggesting a "molecular recognition" mechanism is active in determining LHCII re-distribution upon ST (Allen and Forsberg 2001; Wientjes et al. 2013). Thus, the decreased efficiency of LHCII migration out of grana partitions in *ΔLhca* might be explained by the lack of LHCI, namely lack of digitonin-sensitive binding site for LHCII to PSI. In wild type, the existence of these sites yields into effective quenching of extra LHCII in both margins and stroma lamellae, while only LHCII bound to the PsaH side is efficiently quenched in the mutant. Even though mutant upregulates the formation of PSI–LHCII$_{n=1}$ supercomplexes, this effect is insufficient to match the level of F_m'' quenching obtained with wild-type plants.

Overall, these results suggest that the existence of LHCI-binding site is instrumental in promoting P-LHCII migration to PSI. Moreover, it comes that caution should be applied to RT Chl fluorescence analysis of ST (Jensen et al. 2000) when thylakoid architecture is significantly modified by mutation or when comparing species with different distributions of LHCII between thylakoid domains (Pinnola et al. 2015).

Acknowledgements This research was supported by the Marie Curie Actions—Networks for Initial Training Accliphot (PITN-2012-316427) and SE2B (675006-SE2B), and by HuntingLight/University of Verona.

Author contributions M.B. isolated single knock-out *Arabidopsis* mutants, carried out the crossings, and performed the biochemical and physiological characterization of their photosynthetic apparatus. L.D. measured state I–state II transitions and performed data analysis. R.B. and L.D. conceived the investigation, took part in its design and coordination, and wrote the manuscript.

References

Allen JF (1992) Protein phosphorylation in regulation of photosynthesis. Biochim Biophys Acta 1098:275–335

Allen JF, Forsberg J (2001) Molecular recognition in thylakoid structure and function. Trends Plant Sci 6:317–326

Amunts A, Toporik H, Borovikova A, Nelson N (2010) Structure determination and improved model of plant Photosystem I. J Biol Chem 285:3478–3486

Anderson JM (1986) Photoregulation of the composition, function and structure of thylakoid membranes. Ann Rev Plant Physiol 37:93–136

Ballottari M, Govoni C, Caffarri S, Morosinotto T (2004) Stoichiometry of LHCI antenna polypeptides and characterisation of gap and linker pigments in higher plants Photosystem I. Eur J Biochem 271:4659–4665

Ballottari M, Dall'Osto L, Morosinotto T, Bassi R (2007) Contrasting behavior of higher plant photosystem I and II antenna systems during acclimation. J Biol Chem 282:8947–8958

Barbato R, Bergo E, Szabo I, Dalla Vecchia F, Giacometti GM (2000) Ultraviolet B exposure of whole leaves of barley affects structure and functional organization of photosystem II. J Biol Chem 275:10976–10982

Bell AJ, Frankel LK, Bricker TM (2015) High yield non-detergent isolation of Photosystem I-Light harvesting chlorophyll II membranes from spinach thylakoids. Implications for the organization of the PS I antennae in higher plants. J Biol Chem 290:18429–18437

Bellafiore S, Barneche F, Peltier G, Rochaix JD (2005) State transitions and light adaptation require chloroplast thylakoid protein kinase STN7. Nature 433:892–895

Benson SL, Maheswaran P, Ware MA, Hunter CN, Horton P, Jansson S, Ruban AV, Johnson MP (2015) An intact light harvesting complex I antenna system is required for complete state transitions in Arabidopsis. Nat Plants 1:15176

Betterle N, Ballottari M, Baginsky S, Bassi R (2015) High light-dependent phosphorylation of photosystem II inner antenna CP29 in monocots is STN7 independent and enhances nonphotochemical quenching. Plant Physiol 167:457–471

Bos I, Bland KM, Tian L, Croce R, Frankel LK, Van Amerongen H, Bricker TM, Wientjes E (2017) Multiple LHCII antennae can transfer energy efficiently to a single Photosystem I. Biochim Biophys Acta 1858:371–378

Bressan M, Dall'Osto L, Bargigia I, Alcocer MJP, Viola D, Cerullo G, D'Andrea C, Bassi R, Ballottari M (2016) LHCII can substitute for LHCI as an antenna for Photosystem I but with reduced light harvesting capacity. Nat Plants 2:16131

Casazza AP, Tarantino D, Soave C (2001) Preparation and functional characterization of thylakoids from *Arabidopsis thaliana*. Photosynth Res 68:175–180

Cazzaniga S, Bressan M, Carbonera D, Agostini A, Dall'Osto L (2016) Differential roles of carotenes and xanthophylls in photosystem I photoprotection. BioChemistry 55:3636–3649

Chuartzman S, Nevo R, Shimoni E, Charuvi D, Kiss V, Ohad I, Brumfeld V, Reich Z (2008) Thylakoid membrane remodeling during state transitions in Arabidopsis. Plant Cell 20:1029–1039

Crepin A, Caffarri S (2015) The specific localizations of phosphorylated Lhcb1 and Lhcb2 isoforms reveal the role of Lhcb2 in the formation of the PSI-LHCII supercomplex in Arabidopsis during state transitions. Biochim Biophys Acta 1847:1539–1548

Dall'Osto L, Unlu C, Cazzaniga S, Van Amerongen H (2014) Disturbed excitation energy transfer in *Arabidopsis thaliana* mutants lacking minor antenna complexes of photosystem II. Biochimica Biophysica Acta 1837:1981–1988

Dall'Osto L, Bressan M, Bassi R (2015) Biogenesis of light harvesting proteins. Biochimica Biophysica Acta 1847:861–871

de Bianchi S, Dall'Osto L, Tognon G, Morosinotto T, Bassi R (2008) Minor antenna proteins CP24 and CP26 affect the interactions between photosystem II subunits and the electron transport rate in grana membranes of Arabidopsis. Plant Cell 20:1012–1028

Delosme R, Olive J, Wollman F-A (1996) Changes in light energy distribution upon state transitions: an in vivo photoacoustic study of the wild type and photosynthesis mutants from *Chlamydomonas reinhardtii*. Biochim Biophys Acta 1273:150–158

Engelmann E, Zucchelli G, Garlaschi FM, Casazza AP, Jennings RC (2005) The effect of outer antenna complexes on the photochemical trapping rate in barley thylakoid Photosystem II. Biochimica Biophysica Acta 1706:276–286

Galka P, Santabarbara S, Khuong TTH, Degand H, Morsomme P, Jennings RC, Boekema EJ, Caffarri S (2012) Functional analyses of the plant photosystem I–Light-harvesting complex II supercomplex reveal that Light-harvesting complex II loosely bound to Photosystem II is a very efficient antenna for Photosystem I in state II. Plant Cell 24:2963–2978

Ganeteg U, Kulheim C, Andersson J, Jansson S (2004) Is each light-harvesting complex protein important for plant fitness? Plant Physiol 134:502–509

Gilmore AM, Yamamoto HY (1991) Zeaxanthin formation and energy-dependent fluorescence quenching in pea chloroplasts under artificially mediated linear and cyclic electron transport. Plant Physiol 96:635–643

Horton P, Ruban AV, Walters RG (1996) Regulation of light harvesting in green plants. Annu Rev Plant Physiol Plant Mol Biol 47:655–684

Jansson S (1999) A guide to the Lhc genes and their relatives in Arabidopsis. Trends Plant Sci 4:236–240

Jansson S, Andersen B, Scheller HV (1996) Nearest-neighbor analysis of higher-plant photosystem I holocomplex. Plant Physiol 112:409–420

Jarvi S, Suorsa M, Paakkarinen V, Aro E-M (2011) Optimized native gel systems for separation of thylakoid protein complexes: novel super- and mega-complexes. Biochem J 439:207–214

Jensen PE, Gilpin M, Knoetzel J, Scheller HV (2000) The PSI-K subunit of photosystem I is involved in the interaction between light-harvesting complex I and the photosystem I reaction center core. J Biol Chem 275:24701–24708

Klimmek F, Ganeteg U, Ihalainen JA, van Roon H, Jensen PE, Scheller HV, Dekker JP, Jansson S (2005) The structure of higher plant LHCI: in vivo characterisation and structural interdependence of the Lhca proteins. Biochemisty 44:3065–3073

Laemmli UK (1970) Cleavage of structural proteins during the assembly of the head of bacteriophage T4. Nature 227:680–685

Lam E, Ortiz W, Malkin R (1984) Chlorophyll a/b proteins of photosystem I. FEBS Lett 168:10–14

Leoni C, Pietrzykowska M, kiss AZ, Suorsa M, Ceci LR, Aro E-M, Jansson S (2013) Very rapid phosphorylation kinetics suggest a unique role for Lhcb2 during state transitions in Arabidopsis. Plant J 76:236–246

Liu Z, Yan H, Wang K, Kuang T, Zhang J, Gui L, An X, Chang W (2004) Crystal structure of spinach major light-harvesting complex at 2.72 A resolution. Nature 428:287–292

Lunde C, Jensen PE, Haldrup A, Knoetzel J, Scheller HV (2000) The PSI-H subunit of photosystem I is essential for state transitions in plant photosynthesis. Nature 408:613–615

Mazor Y, Borovikova A, Nelson N (2015) The structure of plant photosystem I super-complex at 2.8 Å resolution. Elife 4:e07433

Nelson N, Ben Shem A (2004) The complex architecture of oxygenic photosynthesis. Nature 5:1–12

Pan X, Li M, Wan T, Wang L, Jia C, Hou Z, Zhao X, Zhang J, Chang W (2011) Structural insights into energy regulation of light-harvesting complex CP29 from spinach. Nat Struct Mol Biol 18:309–315

Pesaresi P, Hertle A, Pribil M, Kleine T, Wagner R, Strissel H, Ihnatowicz A, Bonardi V, Scharfenberg M, Schneider A, Pfannschmidt T, Leister D (2009) Arabidopsis STN7 kinase provides a link between short- and long-term photosynthetic acclimation. Plant Cell 21:2402–2423

Pesaresi P, Hertle A, Pribil M, Schneider A, Kleine T, Leister D (2010) Optimizing photosynthesis under fluctuating light. Plant Signaling Behav 5:21–25

Pesaresi P, Pribil M, Wunder T, Leister D (2011) Dynamics of reversible protein phosphorylation in thylakoids of flowering plants: The roles of STN7, STN8 and TAP38. Biochimica et Biophysica Acta-Bioenergetics 1807:887–896

Peter GF, Takeuchi T, Thornber JP (1991) Solubilization and two-dimensional electrophoretic procedures for studying the organization and composition of photosynthetic membrane polypeptides. Methods 3:115–124

Pinnola A, Cazzaniga S, Alboresi A, Nevo R, Levin-Zaidman S, Reich Z, Bassi R (2015) Light-harvesting complex stress-related proteins catalyze excess energy dissipation in both photosystems of physcomitrella patens. Plant Cell 27:3213–3227

Pribil M, Pesaresi P, Hertle A, Barbato R, Leister D (2010) Role of plastid protein phosphatase TAP38 in LHCII dephosphorylation and thylakoid electron flow. PLoS Biol 8:1–12

Qin X, Suga M, Kuang T, Shen J-R (2015) Structural basis for energy transfer pathways in the plant PSI-LHCI supercomplex. Science 348:989–995

Ruban AV, Wentworth M, Yakushevska AE, Andersson J, Lee PJ, Keegstra W, Dekker JP, Boekema EJ, Jansson S, Horton P (2003) Plants lacking the main light-harvesting complex retain photosystem II macro-organization. Nature 421:648–652

Ruban AV, Johnson MP, Duffy CD (2012) The photoprotective molecular switch in the photosystem II antenna. Biochim Biophys Acta 1817:167–181

Schägger H, von Jagow G (1987) Tricine-sodium dodecyl sulfate-polyacrylamide gel electrophoresis for the separation of proteins in the range from 1 to 100 kDa. Anal Biochem 166:368–379

Tikkanen M, Nurmi M, Suorsa M, Danielsson R, Mamedov F, Styring S, Aro E-M (2008) Phosphorylation-dependent regulation of excitation energy distribution between the two photosystems in higher plants. Biochim Biophys Acta 1777:425–432

Unlu C, Drop B, Croce R, Van Amerongen H (2014) State transitions in Chlamydomonas reinhardtii strongly modulate the functional size of photosystem II but not of photosystem I. Proc Nat Ac Sciences USA 111:3460–3465

Wientjes E, Drop B, Kouril R, Boekem EJ, Croce R (2013) During state 1 to state 2 transition in *Arabidopsis thaliana*, the photosystem II supercomplex gets phosphorylated but does not disassemble. J Biol Chem 288:32821–32826

Yadav KN, Semchonok DA, Nosek L, Kouril R, Fucile G, Boekema EJ, Eichacker L (2017) Supercomplexes of plant Photosystem I with cytochrome b6f, Light-harvesting complex II and NDH. Biochim Biophys Acta 1858:12–20

Zhang S, Scheller HV (2004) Light-harvesting complex II binds to several small subunits of photosystem I. J Biol Chem 279:3180–3187